FULL PAPER

xxxx

**ADVANCED
MATERIALS
INTERFACES**

www.advmatinterfaces.de

One Step Process for Infiltration of Magnetic Nanoparticles into CNT Arrays for Enhanced Field Emission

Srividya Sridhar, Chandra Sekhar Tiwary, Benjamin Sirota, Sehmus Ozden, Kaushik Kalaga, Wongbong Choi, Robert Vajtai, * *Krisztian Kordas,* * and *Pulickel M. Ajayan* *

The complexities and functionalities of carbon nanotube (CNT) architectures can be enhanced even further by the addition of nanoparticles of different kinds. Here, a simple and easily scalable energy efficient infiltration technique is demonstrated to incorporate iron oxide (Fe_3O_4) particles into aligned forests of CNTs grown by chemical vapor deposition. Scanning electron microscopy and in situ confocal microscopy confirm the presence of Fe_3O_4 and also explain the mechanism of infiltration and entrapment in the nanotube films. The obtained hybrid films are demonstrated to be excellent field emitters. The infiltration of nanoparticle results in an order of magnitude improvement in the turn-on field, which can be attributed to several advantageous factors such as reduced screening effects, improved conductivity, and local electric field enhancement in the proximity of the particles. The present method is generic and thus can be applied to other magnetic particles and porous host materials aiming at innovative sensor, electrical and environmental applications.

1. Introduction

Carbon nanotubes (CNTs) due to their fascinating mechanical, electrical, thermal, and optical properties[1–4] have emerged as promising candidates for a number of different nanoscale electronic devices.[5–9] In order to innovative their properties

Dr. S. Sridhar, Dr. C. S. Tiwary, Dr. S. Ozden, Dr. K. Kalaga,
Dr. R. Vajtai, Prof. P. M. Ajayan
Department of Materials Science and NanoEngineering
Rice University
Houston, TX 77005, USA
E-mail: Robert.Vajtai@rice.edu; ajayan@rice.edu
Dr. C. S. Tiwary
Materials Science and Engineering
Indian Institute of Technology
Gandhinagar, India
Dr. B. Sirota, Prof. W. Choi
Department of Material Science and Engineering
University of North Texas
Denton, TX 76203, USA
Prof. K. Kordas
Microelectronics Research Unit
University of Oulu
P.O. Box 4500, FI-90014 Oulu, Finland
E-mail: krisztian.kordas@oulu.fi

(iD) The ORCID identification number(s) for the author(s) of this article can be found under https://doi.org/10.1002/admi.201701631.

(optical, electrical, magnetic, chemical, and mechanical) even further, modifications by the means of encapsulation[10–13] and surface anchoring of nanoparticles of metals and metal oxides are reported.[14–19] Many efforts have been devoted to decorating CNTs with diverse materials by either covalent or van der Waals attachment as well as by polymer wrapping.[20] Among the various nanocomposites, magnetic CNT composites made of iron/iron oxide nanoparticles were suggested to be of great importance because of their potential uses in magnetic data storage, xerography, biosensors, microwave absorbing materials and in magnetic force microscopy.[21–24] In order to synthesize such composites, several methods have been explored, such as electron beam evaporation, chemical vapor deposition, hydrothermal growth, sol–gel synthesis, and conventional impregnation.[14–25] The decoration using most of these processes are multistep and may compromise the intrinsic characteristics of the CNTs.

In this paper, we report an easy, energy efficient, and scalable method to prepare well-aligned CNTs decorated with magnetic particles by using a unique magnetic infiltration technique as shown in the schematic drawing in **Figure 1**. Besides its simplicity, another major advantage of our proposed technique is that the physical structure of the CNTs and the 3D forest alignment remains unaltered. We use in situ confocal microscopy technique to understand the mechanism of such infiltration. Further, we demonstrate stable field-emission of electrons with a tremendous reduction in the turn-on field of devices.[25]

2. Results and Discussion

Figure 2a–c shows SEM images of the CNTs with iron oxide (Fe_3O_4) particles infiltrated using our new method. The vertical alignment and macroscopic structure of the 3D CNT remains unchanged during the process. The SEM images from top and side surfaces reveal the presence of iron oxide particles all around the external surface of the film. From the low magnification SEM image, we can clearly see the way in which the iron oxide nanoparticles are distributed uniformly across the top of the CNT array (marked by the arrow in Figure 2a). As explained in the Experimental Section, the iron oxide particles got infiltrated

**ADVANCED
SCIENCE NEWS**
www.advancedsciencenews.com

**ADVANCED
MATERIALS
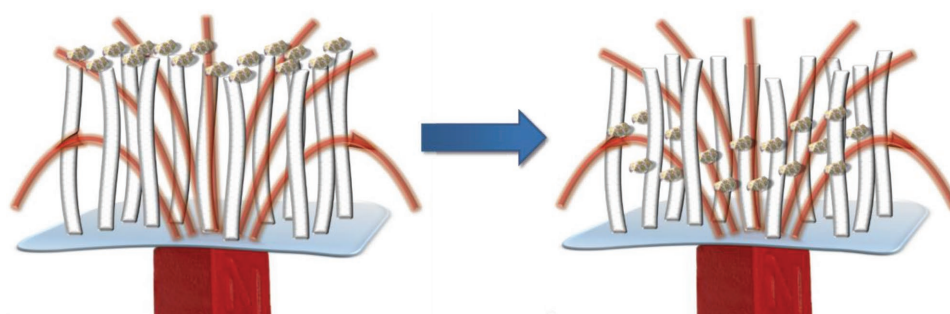INTERFACES**
www.advmatinterfaces.de

Figure 1. Schematic depicting the setup adapted in this work. The vertically aligned carbon nanotube and magnetic nanoparticles dispersed on top, the structure is kept on top of the magnet. After a short duration, the magnetic particles are infiltrated inside the CNT forest.
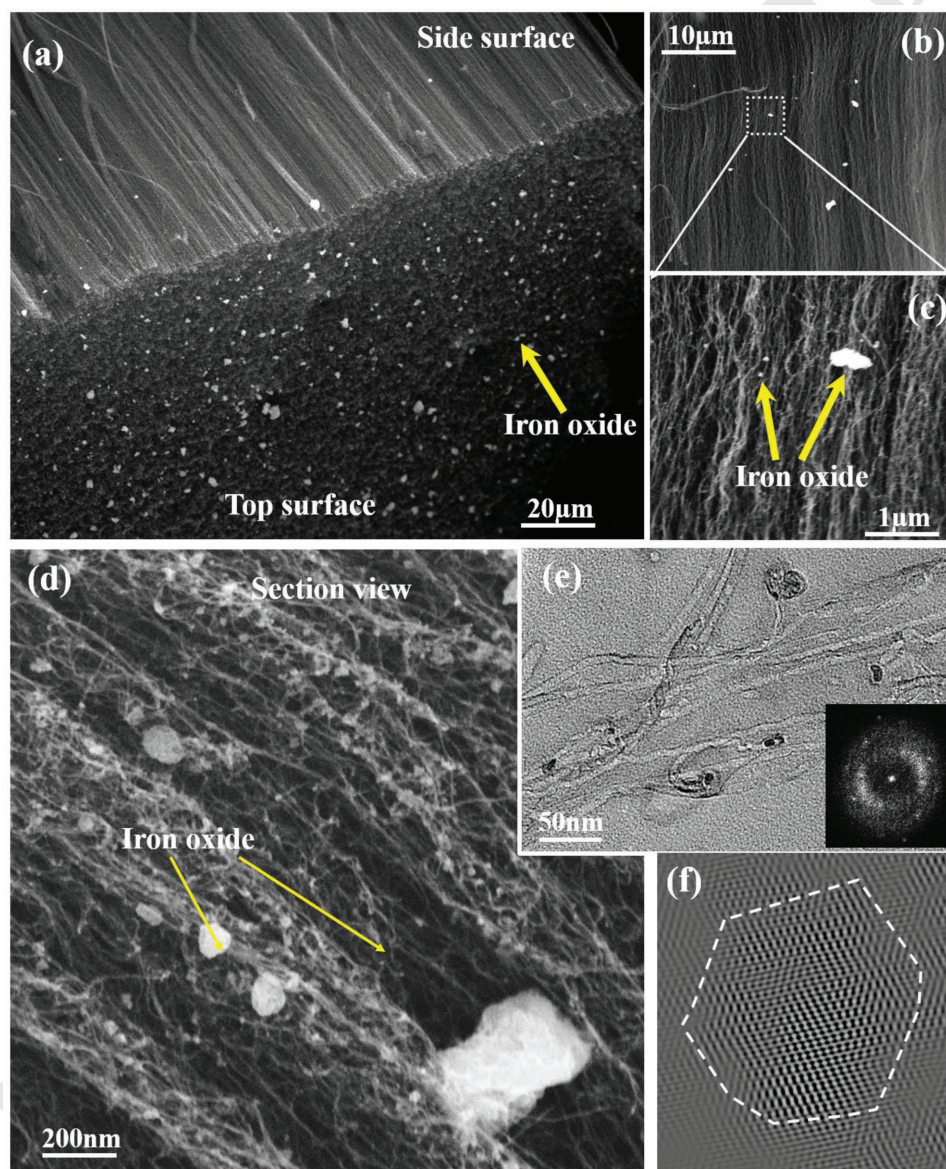

Figure 2. a) Low magnification SEM images of CNT forest in tilted condition to reveal the side and top surface. b) SEM image of the side view and high magnification image selected region c) depicting magnetic particles. d) SEM image after sectioning the forest revealing presence of particles, e) bright field TEM image of particles, and the inset shows FFT of the region. f) Inverse fast Fourier of the particles.
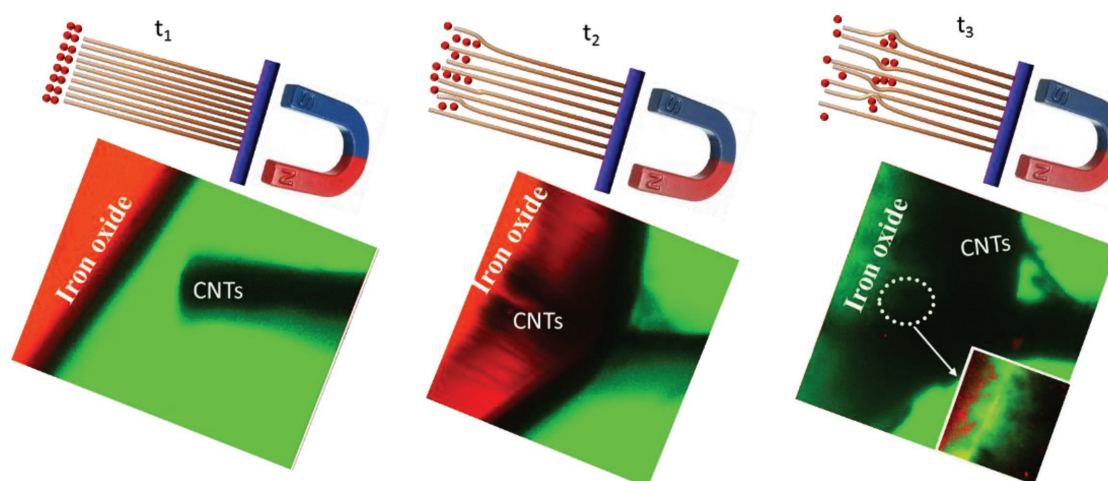
Figure 3. In situ confocal images at different time duration (t1, t2, and t3) of the setup. The schematic on top depicting the observation. The CNT forest in dark and kept on top of the magnet. A high magnification image is shown as an inset.

into the CNTs array with the help of a magnet. We sliced a portion of the CNT forest to observe the cross-sectional view of the array. Figure 2d shows the distribution of submicron size particles across the subsurface. A closer observation of the microstructure reveals the possible mechanism of the inclusion of iron oxide into the CNT forest. The particles appear to be entrapped in the intertubular space of the nanotube film (as also displayed in Figure S1, Supporting Information). The applied magnetic field acts on the ferromagnetic particles and attracts those toward the bulk of the nanotube forest. On the other hand, the cohesion force in-between the long and mechanically flexible nanotubes in the forest makes the host structure to become closed again behind the particles thus facilitating trapping of the iron oxide particles. The SEM image of vertically aligned CNT forest grown on CNTs at two different magnifications is shown in Figure S2 of the Supporting Information. We do not observe any particles or contamination on the surface. Figure 2e shows the TEM observation of the MWCNTs with iron oxide particle trapped between them. The Fast Fourier transformed of the MWCNT with particle is shown as inset. The FFT pattern confirms crystallinity of the particle with the d-spacing that matches with face-centered cubic Fe_3O_4. The inverse Fourier filtered image from these particles shown in Figure 2f confirms the same.

A systematic time dependent in situ confocal imaging using stained ferromagnetic particles was performed to get more in depth understanding of the infiltration mechanism. **Figure 3** shows the schematics as well as the confocal images where the magnetic field was applied for three different time intervals (t1 = 0 min, t2 = 2 min, and t3 = 5 min). The red color staining has been applied to be able to track the infiltration of the nanoparticles dispersion into the black CNT forest. Initially (at time t1), the CNT forest (black color) was placed near to a droplet of highly concentrated colloidal iron oxide dispersion (red color), while the magnet was kept behind the forest (opposite side to iron oxide). After 2 min, we observed an attraction of the magnetic fluid into the CNT forest due to the magnetic field. In subsequent time interval (t3), we observe the stained red particles from the liquid droplet disappeared as they penetrated into the forest. The inset showing a high magnification image confirms the trapping of

these particles in the CNT forest. Please note that, in the low magnification image taken at time t3, the particles are difficult to observe due to their small sizes and black CNT background, although we clearly observe a drastic change in the color of the colloid droplet. The red color particle gets trapped in the black CNT forest and we do not observe red color solution. The time dependent study proves that, as we increase the duration of magnetic interaction, the amount of infiltrated particles increases. Here we should note that, once ferromagnetic particles infiltrate the forest, they further amplify the local magnetic field and thus accelerate the infiltration process. Furthermore, it is worth clarifying that, the current experiments are performed in a horizontal arrangement in order to avoid the gravitational effect.

The pristine and Fe_3O_4 decorated CNT forest grown on the two different substrates (Si and Inconel) were tested for field emission (J vs E) behavior (**Figure 4**). We observe a clear reduction of the turn-on fields (E_{to}) after incorporating Fe_3O_4 particles into the forests. For the samples grown on Si and Inconel E_{to} decreased to 0.3 and 0.2 V μm^{-1}, from 2.8 and 3.3 V μm^{-1}, respectively. The Fowler–Nordheim (F–N) plots displayed in the insets of Figure 4a,b, indicate linear regimes for the large fields, which is often observed for CNT-based field-emitters.[25] Despite the excellent fit, we need to note—since the F–N model has been developed to describe flat metallic surfaces—, one shall use more complex models[27] with additional parameters and statistics that take into account the positions and radii of emitter tips in a network along with their differing work functions CNTs (5.0 eV) and Fe_3O_4 (5.3 eV) making such a calculation to be beyond the scope of this work.

After the field emission experiment, the iron nanoparticles were found to be inside the CNT forest, which was verified, by SEM images taken subsequently (Figure S4, Supporting Information). This proves the fact that once the particles are infiltrated into the CNT forest, they are not disturbed by any physical changes (like tilting or inverting the CNT forest).

As based on current experimental data, it is difficult to probe exact mechanism of the field emission, but based on available literatures, author would like to propose following reason for the current field emission behavior. The role of Fe_3O_4 particles
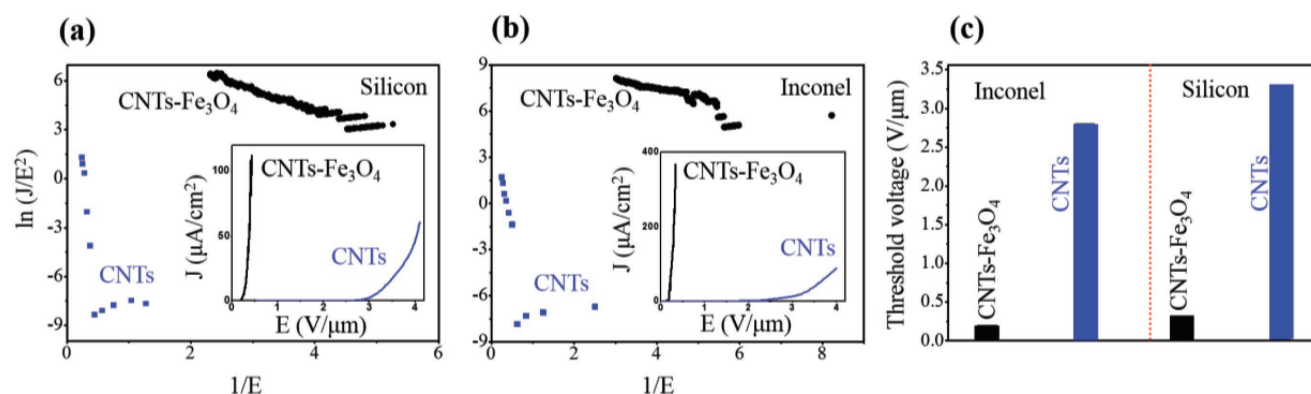
ADVANCED
SCIENCE NEWS
www.advancedsciencenews.com

ADVANCED
MATERIALS
INTERFACES
www.advmatinterfaces.de

Figure 4. ln (J/E^2) versus $1/E$ for CNT forest grown on a) silicon and b) Inconel with and without magnetic particles. J versus E plot of the samples. The blue color is for CNT and the black color for CNT with particles. c) The threshold voltage for various samples.

is manifold in the field-emission enhancement. First, infiltration of Fe_3O_4 nanoparticles results in considerable reduction in the screening effect between the adjacent CNTs. Although, the sharp tips and high aspect ratio are of great advantage for the CNTs to be used as good emitters, the screening effect from the neighboring CNTs compromises these advantages,[28] which is alleviated by the low surface density of Fe_3O_4 particles acting as remote emission centers. Second, the nanoparticles form junctions between CNTs making the percolation path more redundant for the electrons across the forest thus improving the overall conductivity of the films, in accordance with electrochemical impedance spectroscopy measurements on different CNT films (Figure S5, Supporting Information). Third, the infiltrated nanoparticles make intimate physical contact with the CNTs, which may be particularly important, when the emitter surface is not entirely conductive (e.g., because of amorphous carbon on the CNTs) thus electrons would need to tunnel through the insulating layer before emitted to the vacuum. And fourth, Fe_3O_4 has much higher dielectric permittivity than that of vacuum or air, making the concentration of electric field even more efficient in the location of the nanoparticles similar to that demonstrated earlier for CNTs coated with high permittivity $SrTiO_3$.[28] However, a significant benefit of Fe_3O_4 over $SrTiO_3$ is the high electrical conductivity and good electronic band alignment with MWCNTs, making the injection of electrons into nanoparticles more favored.

3. Conclusions

This work demonstrated an easily scalable and simple magnetic method to infiltrate ferromagnetic Fe_3O_4 particles into CNT forests without destructing its physical structure. The infiltration is due to attractive forces acting on the ferromagnetic particles in the magnetic field, which is further promoted by the local field of already inserted particles. After infiltration, the excellent localization and entrapment of the nanoparticles are observed, which is due to the mechanical flexibility and to the presence of cohesive forces within the CNT film. The Fe_3O_4 decorated CNT forests tested in field-emission experiments display an order of magnitude reduced turn-on field as compared to their pristine counterparts owing to the reduced screening effects,

improved conductivity and enhanced electric field localization by the conductive Fe_3O_4 emitters having high dielectric permittivity. The current energy efficient and simple method suggests infiltration of any other magnetic particles in virtually any flexible open pore structure host materials for novel sensors, electronics devices, and environmental applications.

4. Experimental Section

Vertically aligned MWCNTs were grown on Si and Inconel substrates in a water-assisted CVD system. CNTs grown on Si were around 1 cm in height and those grown on Inconel were around of 800 µm in height. Iron oxide (Fe_3O_4) particles were synthesized using chemical precipitation method.[26] 2 mg of these particles was spread across the surface of the CNTs using a spatula. The CNT films with the Fe_3O_4 particles on their top were placed in a Petri dish and then a magnet having a magnetic flux density of ≈0.1 T was brought beneath the container and slowly moved across till most of the nanoparticles got infiltrated inside the CNT array.

The micro and crystal structure of the materials are characterized using scanning electron microscopy (FEI Quanta 400 ESEM FEG), HRTEM (JEOL 2100 F TEM), and Raman spectroscopy (Kaiser Fiber-Optic RAMAN). The in situ confocal microscopy of the process was performed using a Nikon confocal microscope, in order to understand the method of infiltration of nanoparticles into the CNT forest. For this, the iron oxide nanoparticles were mixed with colored dye in water before the infiltration experiments.

After the infiltration of metal nanoparticles; the samples were transferred to a vacuum chamber with a base pressure <10⁻⁶ Torr to conduct field emission measurements. ITO coated with green phosphorous was used as an anode (sample area of 1×1 cm²). The distance between the cathode and the anode was adjusted using a micrometer screw gauge. The CNT tips and the anode were kept ≈500 µm distance apart. The DC voltage was supplied using a Keithley 2410 device. The EIS measurements were performed using a two electrode setup with the CNT on the substrate as the working electrode and lithium metal as the counter/reference electrode. 1 M $LiPF_6$ in 1:1 v/v mixture of ethylene carbonate dimethyl carbonate was used as the electrolyte and glass microfiber filter membrane was used as the separator. The EIS measurements were carried out from 70 kHz to 10 mHz by applying a constant DC bias with a sinusoidal signal of 10 mV.

Supporting Information

Supporting Information is available from the Wiley Online Library or from the author.

[1] M. M. J. Treacy, T. W. Ebbesen, J. M. Gibson, *Nature* **1996**, *381*, 678.

[2] E. W. Wong, P. E. Sheehan, C. M. Lieber, *Science* **1997**, *277*, 1971.

[3] T. W. Ebbesen, H. J. Lezec, H. Hiura, J. W. Bennett, H. F. Ghaemi, T. Thio, *Nature* **1996**, *382*, 54.

[4] H. Dai, J. H. Hafner, A. G. Rinzler, D. T. Colbert, R. E. Smalley, *Nature* **1996**, *384*, 147.

[5] H. Tanaka, S. Akita, L. Pan, Y. Nakayama, *Jpn. J. Appl. Phys.* **2004**, *43*, 864.

[6] M. S. Fuhrer, J. Nygard, L. Shih, M. Forero, Y. G. Yoon, M. S. Mazzoni, H. J. Choi, J. Ihm, S. G. Louie, A. Zettl, P. L. McEuen, *Science* **2000**, *288*, 494.

[7] H. W. C. Postma, T. Teepen, Z. Yao, M. Grifoni, C. Dekker, *Science* **2001**, *293*, 76.

[8] P. G. Collins, M. S. Arnold, P. Avouris, *Science* **2001**, *292*, 706.

[9] S. E. Lyshevski, *Dekker Encyclopedia of Nanoscience and Nanotechnology*, CRC Press, New York **2004**.

[10] J. Bao, Q. Zhou, J. Hong, Z. Xu, *Appl. Phys. Lett.* **2002**, *81*, 4592.

[11] B. K. Pradhan, T. Toba, T. Kyotani, A. Tomita, *Chem. Mater.* **1998**, *10*, 2510.

[12] K. Kordás, T. Mustonen, G. Toth, J. Vähäkangas, A. Uusimäaki, H. Jantunen, A. Gupta, K. V. Rao, R. Vajtai, P. M. Ajayan, *Chem. Mater.* **2007**, *19*, 787.

[13] W. Chen, X. Pan, M.-G. Willinger, D. S. Su, X. Bao, *J. Am. Chem. Soc.* **2006**, *128*, 3136.

[14] J. Li, S. Tang, L. Lu, H. C. Zeng, *J. Am. Chem. Soc.* **2007**, *129*, 9401.

[15] D. R. Kauffman, D. C. Sorescu, D. P. Schofield, B. L. Allen, K. D. Jordan, A. Star, *Nano Lett.* **2010**, *10*, 958.

[16] K. Jiang, A. Eitan, L. S. Schadler, P. M. Ajayan, R. W. Siegel, N. Grobert, M. Mayne, M. Reyes-Reyes, H. Terrones, M. Terrones, *Nano Lett.* **2003**, *3*, 275.

[17] J. Kong, M. G. Chapline, H. Dai, *Adv. Mater.* **2001**, *13*, 1384.

[18] L. Fu, Z. Liu, Y. Liu, B. Han, P. Hu, L. Cao, D. Zhu, *Adv. Mater.* **2005**, *17*, 217.

[19] H. S. Shin, Y. S. Jang, Y. Lee, Y. Jung, S. B. Kim, H. C. Choi, *Adv. Mater.* **2007**, *19*, 2873.

[20] B. Liu, J. Y. Lee, *J. Phys. Chem. B* **2005**, *109*, 23783.

[21] Q. Liu, Z.-G. Chen, B. Liu, W. Ren, F. Li, H. Cong, H.-M. Cheng, *Carbon* **2008**, *46*, 1892.

[22] L. Jiang, L. Gao, *Chem. Mater.* **2003**, *15*, 2848.

[23] Z. Sun, Z. Liu, Y. Wang, B. Han, J. Du, J. Zhang, *J. Mater. Chem.* **2005**, *15*, 4497.

[24] J. Wan, W. Cai, J. Feng, X. Meng, E. Liu, *J. Mater. Chem.* **2007**, *17*, 1188.

[25] S. Sridhar, L. Ge, C. S. Tiwary, A. C. Hart, S. Ozden, K. Kalaga, S. Lei, S. V. Sridhar, R. K. Sinha, H. Harsh, K. Kordas, P. M. Ajayan, R. Vajtai, *ACS Appl. Mater. Interfaces* **2014**, *6*, 1986.

[26] T. N. Narayanan, A. P. Reena Mary, P. K. Anas Swalih, D. Sakthi Kumar, D. Makarov, M. Albrecht, J. Puthumana, A. Anas, M. R. Anantharaman, *J. Nanosci. Nanotechnol.* **2011**, *11*, 1958.

[27] J. He, P. H. Cutler, N. M. Miskovsky, *Appl. Phys. Lett.* **1991**, *59*, 1644.

[28] A. Pandey, A. Prasad, J. P. Moscatello, M. Engelhard, C. Wang, Y. K. Yap, *ACS Nano* **2013**, *7*, 117.

Q7